The ASW Reach-back Cell Ocean Analysis System

J.D. Dykes[1] and P. Fanguy[2]
[1]*Oceanography Division*
[2]*QinetiQ North America*

Introduction: Obtaining a real-time characterization of the 3D structure of the ocean is important in supporting naval operations, particularly in anti-submarine warfare (ASW). The oceanographers and forecasters of the ASW Reach-back Cell (RBC), located at the Naval Oceanographic Office (NAVOCEANO) at Stennis Space Center, Mississippi, analyze ocean and atmospheric data using state-of-the-art computing hardware and software to build a comprehensive picture of the environment in operational areas of interest. Along with the growing technology comes the ever-increasing volume of measurements in the ocean and atmosphere and rapidly expanding data assimilation and numerical modeling prediction capability. These challenging conditions call for a user interface with a concise set of software tools that help the user stay organized and not be overwhelmed by a wide variety of methods and technologies in order to handle the abundance of data. The ASW Reach-back Cell Ocean Analysis System (ARCOAS) is designed to fulfill such requirements.

Software Approach: ARCOAS is a user interface designed on top of ArcMAP version 9.3, a powerful software package using geographic information system (GIS) technology developed by Environmental System Research Institute (ESRI), Inc. A highly flexible programming language used in Microsoft Office applications, Visual Basic for Applications (VBA), is also built into ArcMAP and provides a rapid development path for invoking the powerful GIS functionality of ArcMAP coupled with helpful graphics classes of Microsoft Office components. Thus, ARCOAS is designed and built with an object-oriented approach that incorporates listeners, dialog boxes, interactive displays, and clickable buttons, all put together to offer the user tools tailored to the work at hand. ARCOAS is not just a cleverly coded graphical user interface (GUI) made of classes and modules: it also offers an environment and language in which the oceanographer is familiar and comfortable, while providing environmental information in a common geographic reference frame.

Applications: The primary focus of the oceanographers in the ASW RBC is to assess the level and confidence in the data and model output depicting the current and predicted structure of the ocean. One goal is to provide a level of certainty to other users of the data and model output as it affects their applications (e.g., algorithms for ocean acoustics) and their own interpretations on which critical mission decisions are made. The first step is to quickly locate the data with respect to the Earth, a step at which a GIS is inherently quite proficient. Figure 1 shows a world map view rendering available domains from numerical models such as (1) the global Navy Coastal Ocean Model (NCOM)[1] run at NAVOCEANO; (2) the Coupled Ocean and Atmosphere Mesoscale Prediction System (COAMPS®)[2] run at Fleet Numerical Meteorology and Oceanography Center (FNMOC) in Monterey, California; and (3) WAVEWATCH III[3] run at FNMOC and NRL Stennis. Once located, data can be visualized as shown in Fig. 2, where the view is zoomed to a model domain to focus on the locations of the plotted profiles and the layer rendering the model output of surface water temperature. Other items rendered are (1) locations of environmental measurements such as Expendable Bathythermographs (XBTs) and Argo floats collecting ocean profiles of temperature and salinity; (2) remotely sensed data ground tracks depicting sea surface height (SSH) variations measured by radar altimeters on polar orbiting satellite platforms; and (3) multichannel sea surface temperature (MCSST) data derived from brightness temperatures measured from satellites.

Although Fig. 2 shows a myriad of observation points within this region of interest, further analysis can be performed on specific observation data using a guided process of elimination and selection. Figure 3 shows a plot of measured and modeled time-coincident temperature and salinity profiles at a specific location for comparison. More interesting is the comparison of the overlaid sonic layer depths (SLD) derived from the plotted profiles. SLD is highly sensitive to variations of the thermohaline structure, which directly affects performance of acoustic systems supporting ASW.

Conclusion: Additional capabilities provided in the user-interface structure of ARCOAS include layer mathematics, animations, cross-sections, various drawing functions, a highly configurable setup utility, exporting presentable graphics, and model performance statistics. ARCOAS will serve as a well-tested prototype for further development to increase flexibility by integrating the Department of Defense Commercial Joint Mapping Toolkit (C/JMTK) to build run-time system tools that can be used in other frameworks besides ArcMAP. As we satisfy more functional requirements with further improvements and

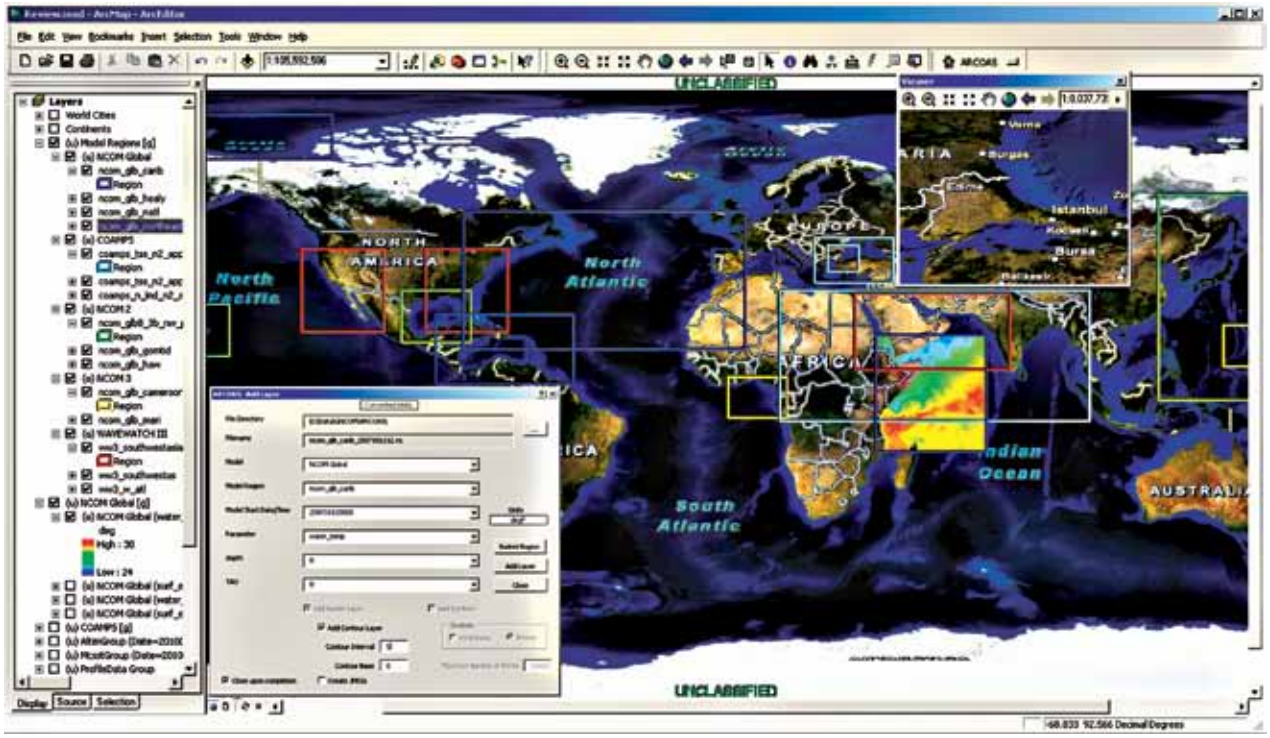

FIGURE 1
Global view of atmospheric and ocean prediction model domains available for analysis. The color-coded boxes correspond to domains organized in groups, in this case by type of model, including global NCOM subsections, COAMPS, and WAVEWATCH III. The table of contents on the left indicates what is displayed. The inset dialog box is the interface for bringing up a data layer from output of a model domain. In this case, a region in the northeastern Indian Ocean was selected and a raster data layer of surface temperature from NCOM is displayed.

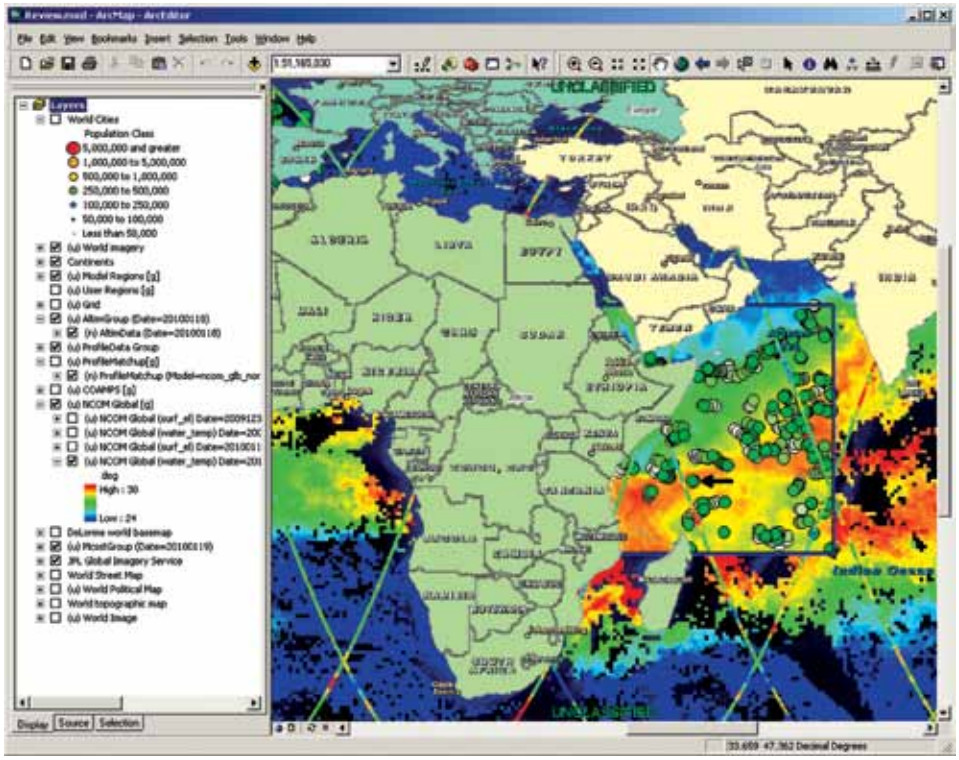

FIGURE 2
A plot of the raster layer referred to in Fig.1 of surface temperature from global NCOM in the northeastern Indian Ocean and the satellite-derived MCSST, showing that they are fairly consistent with each other. Also plotted are the measured SSH variations along ground tracks from a radar altimeter for one day and profile locations limited to the NCOM domain. Greener points are more recent profiles. The selected point indicated by the arrow corresponds to the plots in Fig. 3.

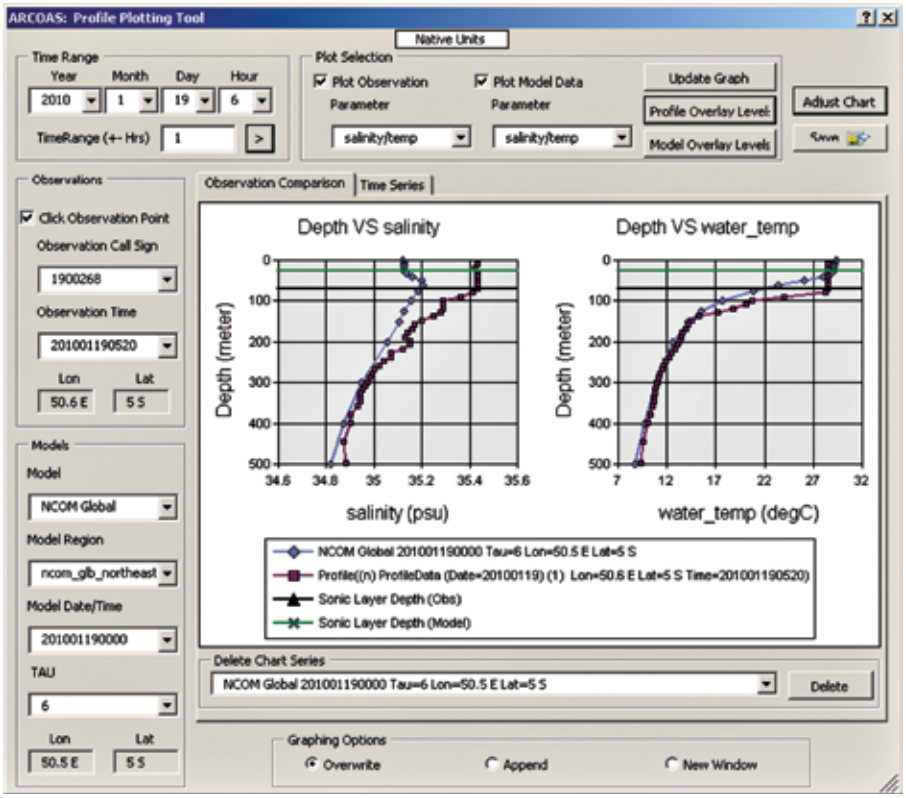

FIGURE 3
Profiles of measured and modeled temperature and salinity plotted from a selected point indicated by the arrow in Fig. 2. The SLD levels overlaid on the profile plots are calculated based on both measured and modeled parameters and show how sensitive SLD is to the ocean thermohaline structure.

follow this new development path, ARCOAS has the potential to be useful for more general meteorological and oceanographic applications in support of Navy operations.

[Sponsored by SPAWAR]

References

[1] C.N. Barron, A.B. Kara, R.C. Rhodes, C. Rowley, and L.F. Smedstad, "Validation Test Report for the 1/8° Global Navy Coastal Ocean Model Nowcast/Forecast System," NRL/MR/7320--07-9019, Naval Research Laboratory, Stennis Space Center, MS, 2007.

[2] R.M. Hodur, "The Naval Research Laboratory's Coupled Ocean/Atmosphere Mesoscale Prediction System (COAMPS)," *Mon. Wea. Rev.* **125**, 1414–1430 (1997).

[3] H.L. Tolman, "Development of a Multi-grid Version of WAVEWATCH III," Tech. Note 256, NOAA/NWS/NCEP/MMAB, 2007.

Marine Sediment Strength from Dynamic Probes

A. Abelev, K.R. Tubbs, and P.J. Valent
Marine Geosciences Division

Background: Rapid assessments of undrained shear strength of marine sediments are often of great interest in various branches of offshore civil and petroleum engineering, and especially for the Navy. Dynamic free-fall penetrometers offer a potential for such rapid strength assessment, but have typically been employed in conjunction with mostly empirical relationships to investigate the undrained shear strengths of sediments. In this work, we analyze the behavior of one such commonly used penetrometer: the STING (Sea Terminal Impact Naval Gauge). It consists of a main sensor assembly with an attached straight shaft of 19 mm diameter and up to 3 m long, with a flat cylindrical plate, called the "foot" hereafter (of several different diameters from 25 to 70 mm) at the rod tip (see Fig. 4). The probe is deployed in free-fall and penetrates foot-first on impact into the sediments (usually soft clayey sediments). The native processing algorithm, based on interpretations of the deceleration time-history of impact, typically suffers from unreliable and inaccurate derivation of the undrained shear strength of sediments — a fundamental strength descriptor, highly important in a wide variety of applications and problems involving marine sediments. An example of using this algorithm is shown in Fig. 4 for a series of drops with different foot diameters at the same location. These data are compared with the standard lab-derived vane test results, representing an accurate measurement of the undrained shear strength of soil. While some records match the lab data well, others deviate significantly, often overpredicting by a factor of five or more. These inconsistencies are typical of a wide range of soils and locations explored.

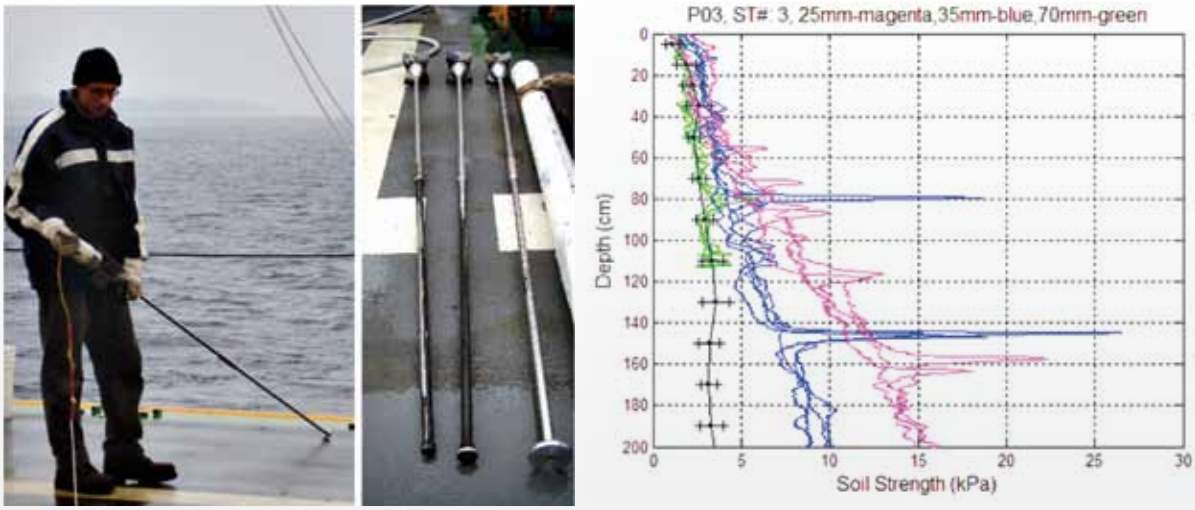

FIGURE 4
(Left to right) STING penetrometer before deployment; several different foot diameters including 25, 35, and 70 mm; and undrained shear strength results from one location processed using STING native algorithms (green, blue, magenta), compared with lab standard vane tests (black curve with error bars representing standard deviation).

Analysis of Bearing Resistance: Analysis of probe impact burial can be conducted using various approaches. One may attempt to produce full dynamic solutions, including large sediment deformation and flow around the penetrating STING, full elasto-plastic constitutive formulations, and rate effects. One such analysis is explored in Ref. 1 using a finite element approach and including ALE (Arbitrary Lagrangian-Eulerian) remeshing scheme. Alternatively, one could use a simplified pseudo-static approach[2] that computes a static collapse load for a pre-embedded STING penetrometer at a series of depths, ranging from the sediment-water interface and down to a depth of about 3 m (maximum STING embedment data available). Although this analysis neglects the effects of prior strains and deformations occurring during the penetration process and assumes the sediment to be at the in situ stress state, it has proven to be useful interpreting penetrations of other probes, such as the XBP (eXpendable Bottom Profiler) probe.

In this work, and similar to that described in Ref. 2, we solve the basic equation of motion, based on the known (and probe-recorded) deceleration time series to derive the overall sediment resistance force, while accounting for buoyancy effects. This sediment resistance force depends strongly on the rate of deformation of the soil, plastically flowing around the penetrating probe.[3,4] We account for these effects using constant coefficients, appropriate to the general materials under consideration, i.e., soft cohesive marine muds. Thus, transitioning from dynamic to pseudo-static sediment force, we approximate the problem of the bearing capacity of foundations, representing the sediment resistance via a nondimensional bearing capacity factor. This factor, in turn, is derived from a series of numerical solutions (pseudo-static) using FLAC3D finite-difference code. These solutions are then represented analytically, by standard curve-fitting, as a function of the foot diameter, embedment depth, and velocity of the probe, allowing for an easy inversion routine to be implemented. An elasto-plastic constitutive model of soil resistance is used, with elastic parameters chosen with utmost care. The single-parameter soil failure model (undrained shear strength) is then derived using the obtained numerical solutions and measured probe decelerations, and adjusted for burial depth and probe velocity. The results of numerical analysis are given in Fig. 5, showing distribution of von Mises (shear) stress and velocity vector and contours of soil, plastically flowing around the penetrating probe. Side friction of soil on the penetrometer rod can be shown to be ignored without major loss of validity. Figure 6 shows the final prediction of the shear strength using original STING software and the new method developed here. Aside from a small initial portion of the curve, the improvement in prediction is significant. Further details of this work can be found in Ref. 5.

Acknowledgments: The help of the crews and research teams in obtaining the field data at sea is greatly appreciated.

[Sponsored by NRL and ONR]

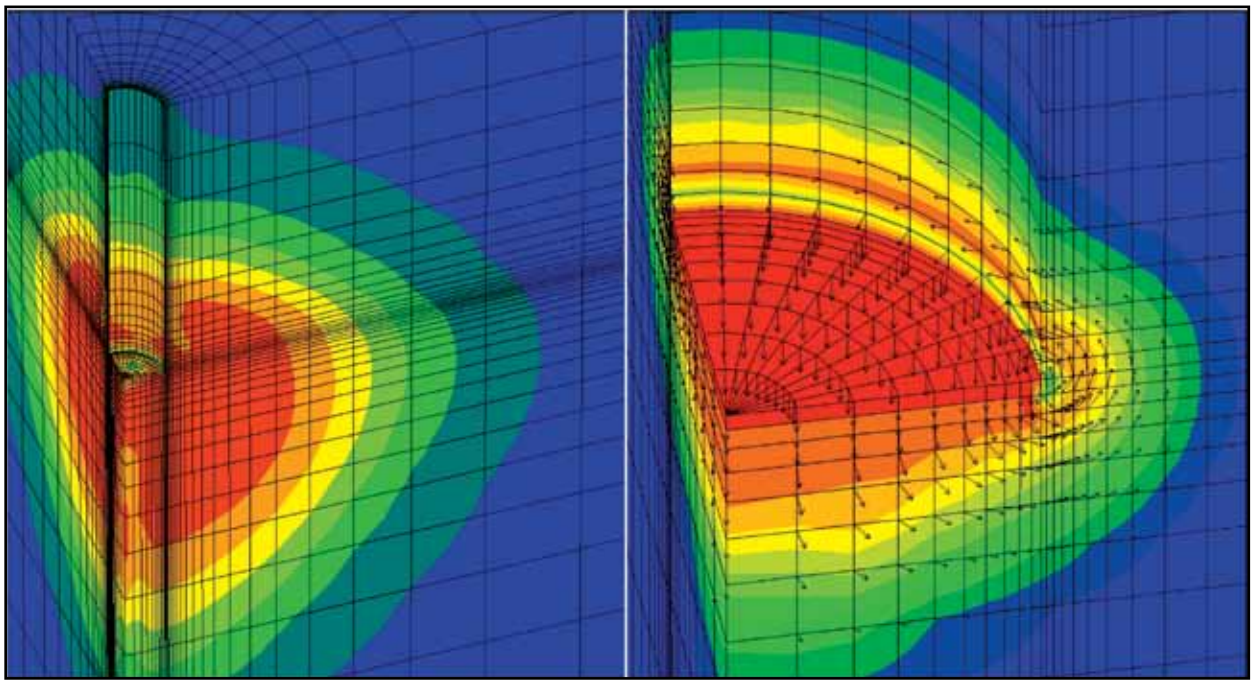

FIGURE 5
Typical results of numerical analysis of STING at a particular embedment depth, showing contours of the von Mises (shear) stress (left) and soil velocity vectors and contours (right), identifying a well-developed failure in the soil and formation of a distinct flow pattern around the foot of the penetrometer.

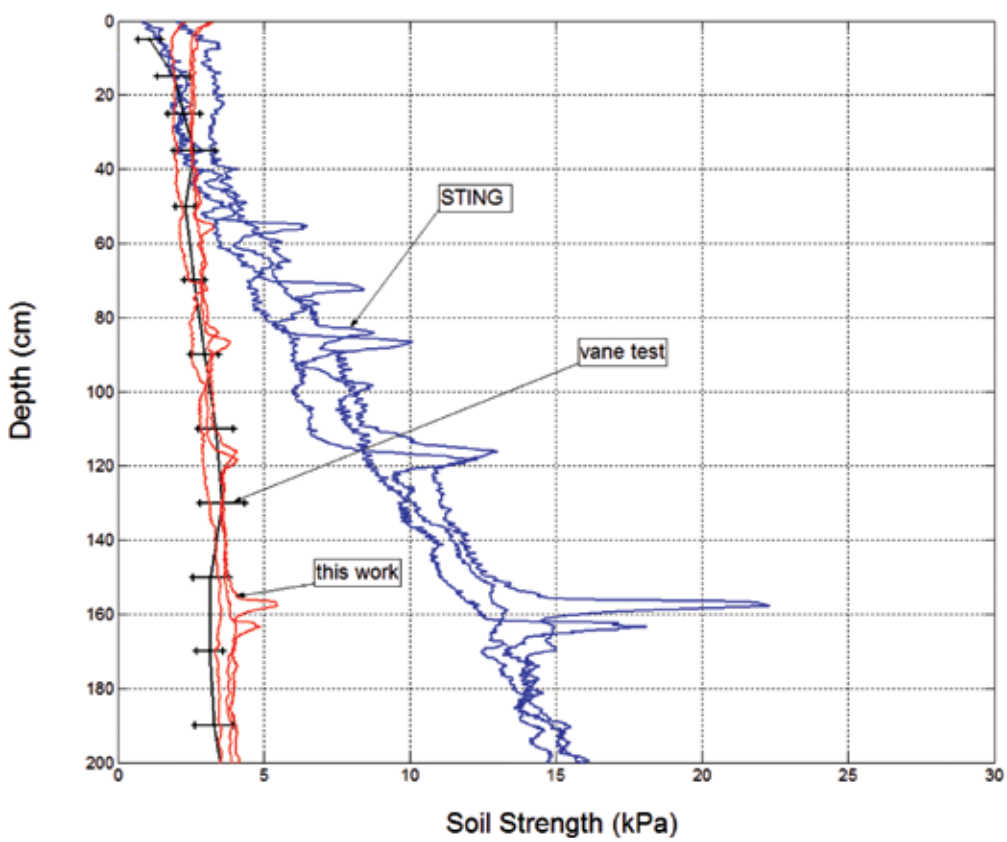

FIGURE 6
STING-processed (blue) and FLAC3D-computed (red) undrained shear strength computation from a location in the Gulf of Mexico, compared with the lab-measured vane test results (black solid lines with error bars representing the standard deviation).

References

[1] A. Abelev, J. Simeonov, and P.J. Valent, "Numerical investigation of Dynamic Free-fall Penetrometers in Soft Cohesive Marine Sediments Using a Finite Element Approach," Oceans 2009, MTS/IEEE Biloxi, MS, 26–29 Oct. 2009, abstract no. 090612-059.

[2] C.P. Aubeny and H. Shi, "Interpretation of Impact Penetration Measurements in Soft Clays," *J. Geotech. Geoenviron. Eng.* **132**, 770 (2006).

[3] C.P. Aubeny and H. Shi, "Effect of Rate-Dependent Soil Strength on Cylinders Penetrating Into Soft Clay," *IEEE J. Ocean. Eng.* **32**, 49–56 (2007).

[4] G. Biscontin and J.M. Pestana, "Influence of Peripheral Velocity on Vane Shear Strength of an Artificial Clay," *Geotech. Testing J.* **24**, 423–429 (2001).

[5] A. Abelev, K. Tubbs, and P.J. Valent, "Numerical Investigation of Dynamic Free-fall Penetrometers in Soft Cohesive Marine Sediments Using a Finite Difference Approach," Oceans 2009, MTS/IEEE Biloxi, MS, 26–29 Oct. 2009, abstract no. 090612-058.

Characterizing River Environments by Combining Imagery and Models: What We Can Do Now and In the Future

C.A. Blain,[1] A.D. Weidemann,[1] R.P. Mied,[2]
R.S. Linzell,[3] and P. McKay[4]
[1]*Oceanography Division*
[2]*Remote Sensing Division*
[3]*QinetiQ North America*
[4]*ASEE Postdoctoral Associate*

The Navy's Push Into Riverine Environments: In response to the increasing use of inland waterways by enemy combatants engaged in the Global War on Terror, the Navy has fielded three new riverine squadrons within the last three years. Their mission involves diverse combinations of surveillance, patrol, interdiction, and delivery of land forces into river environments. This plan to increase the number of river operations highlights the need for detailed descriptions of the water levels, flow, and geometry of a given river.

Rivers pose one of the most challenging environments to characterize because they form the interface between land and water in the coastal margin. They are geometrically complex and change continually in position and character. Predictive models of the river environment require detailed descriptions of river bank position, bed elevation, upstream fluxes, and downstream variability due to tidal modulations. To compound the difficulty, Navy river operations are most often conducted in denied areas across the globe where very little of this information is available.

Meeting the Immediate Challenge: To address the need for a predictive capability for currents and water level in rivers in regions where knowledge of the system is limited, we devised an approach that initiates a river model from available imagery and provides a strategy to compensate for missing data. The River Simulation Tool[1] (RST) provides an intuitive interface for configuring a 2D hydrodynamic model of a river or river segment that has been remotely observed and imaged. In-water points and possible river bank locations are extracted from imagery and processed in such a way as to generate a model grid representing the river bank positions and to derive synthetic bottom depths. The RST defaults to configurations for the river model and contingencies to specify missing information, as necessary, such as upstream forcing or bathymetry. Realizing that a great deal of uncertainty can accompany application of the RST to a real river, a capability for specifying multiple inputs is available. From these multiple data sets, we can perform an ensemble of model runs to bracket the uncertainty or assess the sensitivity of predictions to unknown inputs.

The RST was applied to a segment of the upper East Pearl River in Mississippi, a region having no archived digital shoreline, but for which a Quickbird satellite image is available [Fig. 7(a)]. Applying the RST to the imagery results in an oriented shoreline [Fig. 7(b)] and a model grid with estimated bathymetry [Fig. 7(c)]. In situ data, such as bathymetry, upstream river flux, and downstream tidal variability, are known in this same region, permitting a comparison between river currents and elevation produced by an image-initiated model through the RST [Fig. 8(a)] to observed currents at one location[2] [Fig. 8(b)].

Future Capabilities: In addition to geometric information, color imagery of the river surface contains a rich assortment of features indicative of the underlying flow, such as circulation eddies or mixing zones between different water types. Imagery taken of the Potomac River, Maryland (Fig. 9), shows developing waves that are indicative of an instability between river currents of different magnitudes. Present research efforts aim first to quantify the circulation features in the surface imagery. Sensitivity analyses are then performed by applying an analytical process model to the same river reach to better understand the relationship between the surface circulation and the 3D structure of the river currents. A relationship between surface currents and 3D river currents can ultimately be used to formulate a methodology for constraining modeled river flow based on surface imagery. Such a leap in technology dramatically enhances our ability to address the needs of mission planners for riverine operations through more accurate representations of actual riverine environments.

[Sponsored by NRL and SPAWAR]

FIGURE 7
The RST is applied to the lower east Pearl River, MS. (a) Multispectral imagery from the Quickbird satellite taken on May 1, 2007; (b) shoreline coordinates processed from water points and edge data extracted from imagery; (c) the resulting 2D river model created by the RST with color contours indicating water depth.

(a)

(b)

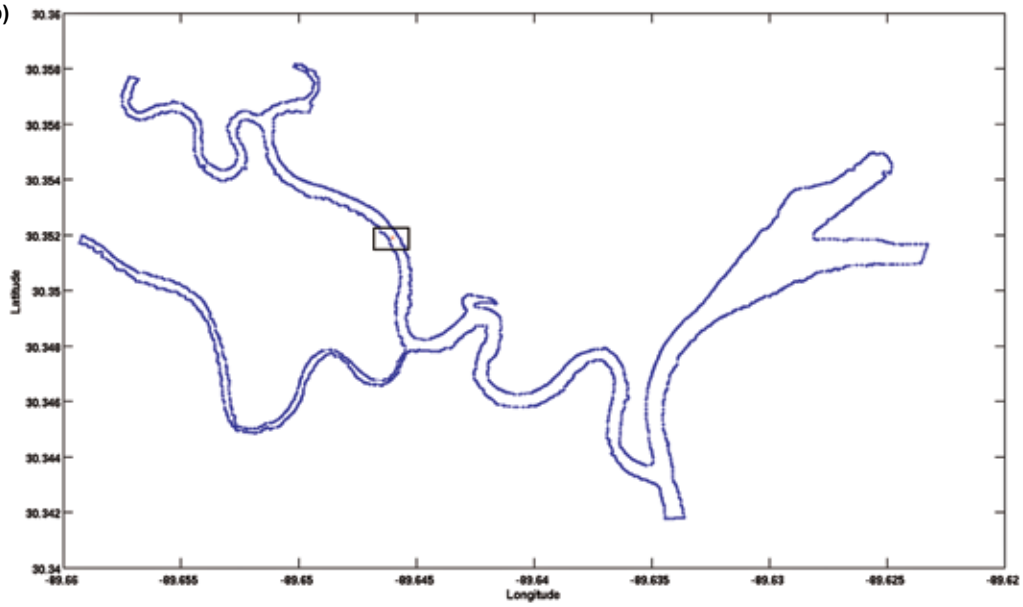

(c)

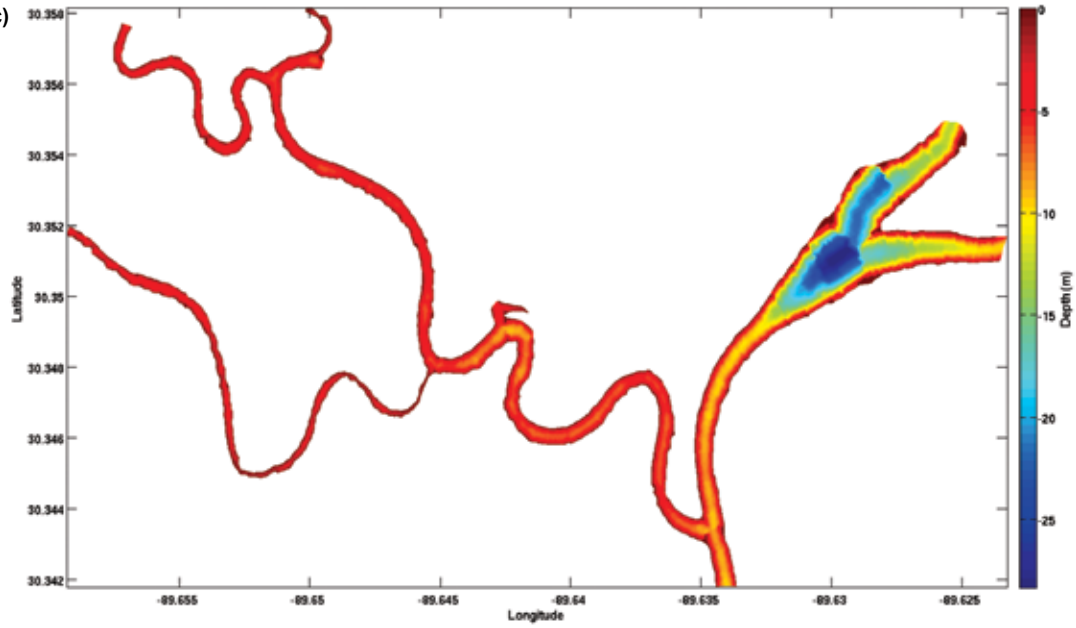

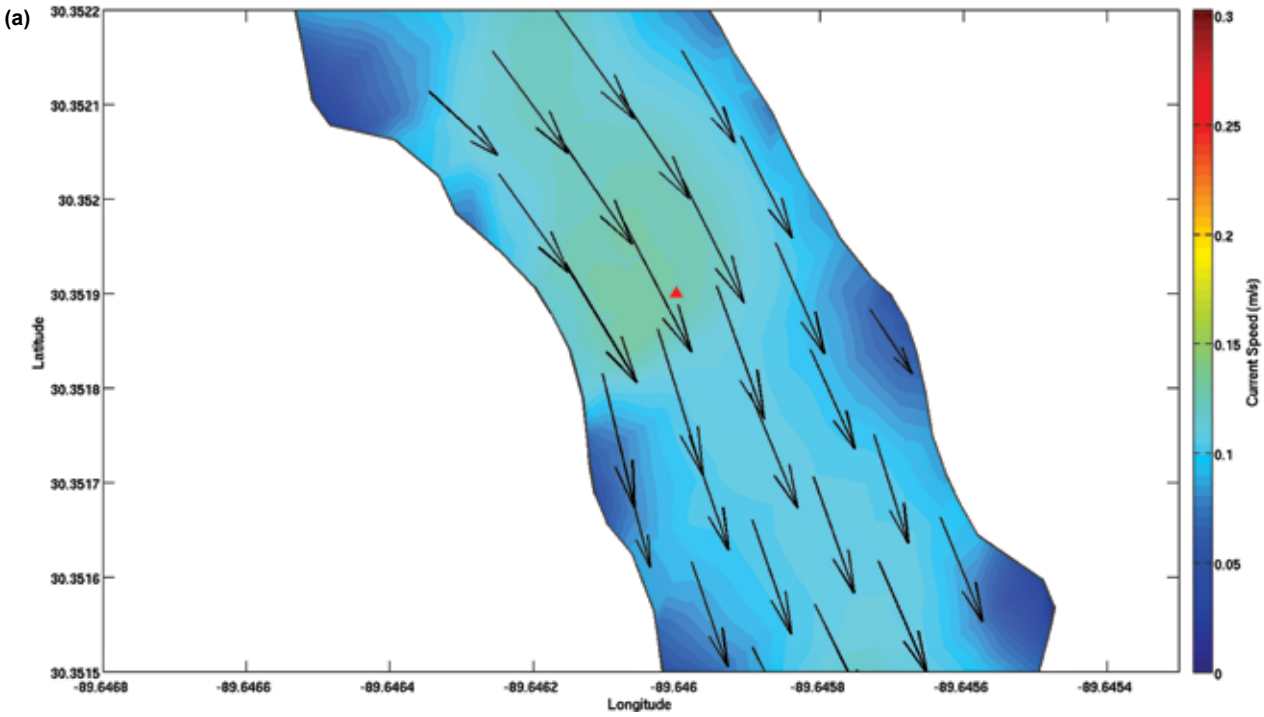

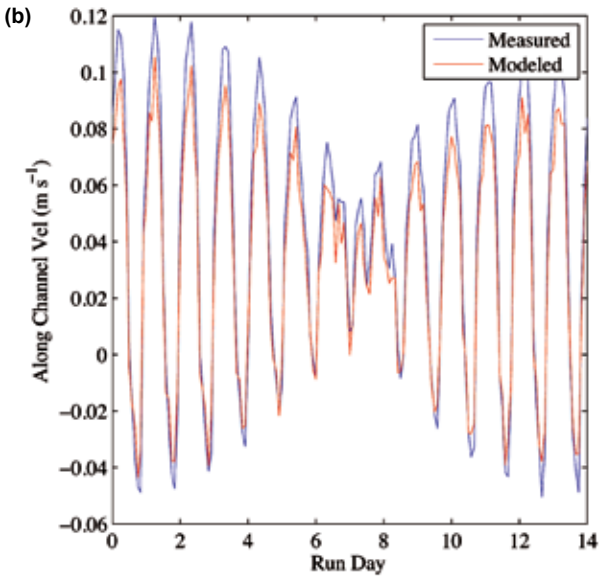

FIGURE 8
Modeled currents from the RST within a single river reach: shown are (a) the magnitude as color, and direction as arrows; and (b) a comparison to measured currents at one location.

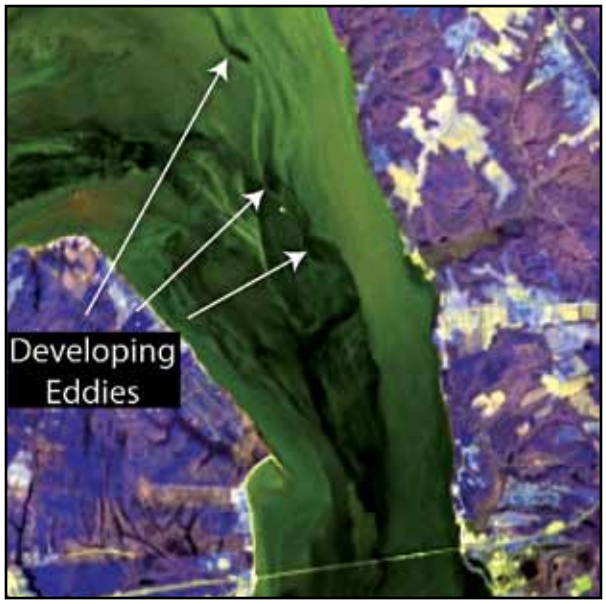

FIGURE 9
Imagery at a bend in the Potomac River, MD, taken by the ASTER satellite on April 2, 2003.

References

[1] C.A. Blain, R. Linzell, A. Weidemann, and P. Lyon, "A Tool for Rapid Configuration of a River Model," MTS/IEEE Oceans'09 Conference Proceedings, Biloxi, MS, Oct. 28, 2009.

[2] P. McKay and C.A. Blain, "Toward Developing a Hydrodynamic Flow and Inundation Model of the Lower Pearl River," MTS/IEEE Oceans'09 Conference Proceedings, Biloxi, MS, Oct. 28, 2009.